

Probing axion and muon-philic new physics with muon beam dump

Haotian Li,^{1,*} Zuowei Liu,^{1,†} and Ningqiang Song^{2,‡}

¹*Department of Physics, Nanjing University, Nanjing 210093, China*

²*Institute of Theoretical Physics, Chinese Academy of Sciences, Beijing, 100190, China*

(Dated: January 14, 2025)

High-energy muon beam dump experiments are powerful probes of new physics models beyond the Standard Model, particularly those involving muon-philic interactions. In this study, we place constraints on three new physics models utilizing data from the recent NA64 μ experiment: (1) axions coupling to photons, (2) axions coupling to muons, and (3) a muon-philic dark sector mediated by a massless $U(1)_{L_\mu-L_\tau}$ gauge boson. A key signature of these models is the significant missing energy from the production of new particles that either escape the downstream detectors or decay between them. We find that the current NA64 μ data do not yet probe new parameter region on axion-photon coupling. For muon-philic axions, the current NA64 μ data can exclude new parameter space for the axion-muon coupling $g_{a\mu\mu} \gtrsim 4 \times 10^{-3} \text{ GeV}^{-1}$ and the axion mass $m_a \lesssim 0.2 \text{ GeV}$. For a muon-philic dark sector, the current data provide stringent constraints that surpass existing ones by nearly one order of magnitude. The data from 2023 NA64 μ run, once available, will be capable of excluding new axion-photon coupling parameter space and examine the axion explanation of muon $g-2$ deviation, with more sensitivity advancement expected in near future runs.

I. INTRODUCTION

While the Standard Model (SM) has achieved remarkable success, it fails to explain several key observations, in particular, the existence of dark matter. The extension of SM involves the introduction of new particles or a dark sector. Among them, QCD axion has drawn increasing attention due to its capability of solving the strong CP problem with a spontaneously broken global $U(1)$ Peccei-Quinn symmetry [1–4]. Axions can be produced from the misalignment mechanism and constitute the cosmological dark matter [5–12]. String theories also predict a copious amount of axions in our Universe [13–15].

Similar to QCD axion, axion-like particles (ALPs) are pseudoscalar particles coupling to SM gauge bosons or fermions. Without a definite relation between the mass and the coupling to the SM, ALPs typically do not solve the strong CP problem, but remain as good dark matter candidates [9]. In light of this similarity, we use axion and ALP interchangeably in this work. Axions are constrained from terrestrial haloscopes (e.g. [16–18]), beam dump and collider experiments (e.g. [19–21]) and astrophysical observations (e.g. [22–24]).

Recently, Fermilab announced the updated measurements of muon anomalous magnetic moment [25] with improved precision compared with Run-1 results [26], which show substantial tension with the SM prediction [27]. Although the hadronic contribution from lattice calculation leads to a much smaller deviation from the measurement [28, 29], it is still imperative to explore the new physics possibilities in muon $g-2$. ALPs with muon coupling have been a promising explanation for the anomaly [30–35]. We will examine the possibility in this work.

Apart from axions, a natural extension of the SM is a dark sector with a $U(1)$ gauge group. The dark sector is weakly coupled to the SM by introducing kinetic mixing terms [36, 37] between SM gauge bosons and

the new $U(1)$ gauge boson, the so-called “dark photon”. The kinetic mixing may arise through a variety of ways, in particular through loops of heavy particles that are charged under both SM and new $U(1)$ gauge symmetries [36, 38, 39]. For massless dark photon, the kinetic mixing can be removed through the redefinition of the gauge field, when dark sector particles couple weakly to SM gauge bosons and appear to be “millicharged particles” [40]. Searches for millicharged particles have been conducted in electron and proton [41–44] beam dumps, collider experiments [45–49], and through cosmic rays secondaries at neutrino experiments [50–55].

Despite the extensive study of axions and the dark sector, the direct probe of flavor-specific new physics has only been available recently with the NA64 μ experiment [56, 57], where a muon beam is dumped onto the target to search for missing energy. New runs have been made in 2023 to increase the number of muons. Although the electroweak interaction in the SM is flavor independent, flavor non-universality is generally expected in supersymmetry and flavored Higgs models [58–61]. In particular, lepton flavor non-universality has been studied in the context of non-standard neutrino interactions [62, 63] and flavor-violating interactions [33, 64–66]. Therefore, a muon beam dump is one of the superior ways of probing muon-philic new physics, and it is timely to investigate the current status of new physics and the potential with NA64 μ .

In this work, we explore three new physics scenarios illustrated in Fig. 1: 1) axion coupling to photons, 2) axion coupling to muons, and 3) a dark sector interacting with muon through massless $U(1)_{L_\mu-L_\tau}$ gauge boson, which appears to be millicharged in other beam dump experiments. We derive the corresponding constraints on dark particles with mass below GeV by investigating the missing energy events at the NA64 μ experiment, which cover a large parameter space that was unexplored before. The sensitivity will be further improved in ongoing searches

with higher muon luminosity.

II. THE NEW PHYSICS SIGNALS AT NA64 μ

The NA64 μ experiment is conducted at CERN using the M2 beam line. The muon beam (with the momentum of 160 ± 3 GeV) from the proton dump is selected and collimated to be incident on the target, which is the electromagnetic calorimeter (ECAL) consisting of lead and plastic scintillator layers [56, 57]. After exiting ECAL, the muon traverses the veto counter, hadronic calorimeter (VHCAL), muon trackers and finally two large hadronic calorimeters (HCALs). We use the data sample taken at NA64 μ in May 2022 [56]. The data are recorded as the calorimeter-deposited energy (E_{cal}) and the outgoing muon momentum (p_{out}), where different categories of events lie in different regions of the $E_{\text{cal}} - p_{\text{out}}$ plane. We choose the signal region $p_{\mu, \text{out}} < 120$ GeV and $E_{\text{CAL}} < 12$ GeV. This is the region where large missing energy is not recorded in the detector. No events are observed [56] in this region and the expected number of SM background events is also much less than 1, which can be safely neglected. However, if the scattering produces beyond-the-Standard-Model (BSM) particles that carry a significant amount of the incoming muon energy and subsequently escape from the calorimeters, the BSM signal may fall in this region.

As depicted in Fig. 1, we consider the production of dark particle through bremsstrahlung-like process at NA64 μ . The expected number of BSM events is generally computed by

$$N_{\text{signal}} = N_{\text{MOT}} n_{\text{Pb}} L_T \int d\sigma(\mu N \rightarrow \mu N X) \kappa P_{\text{inv}}, \quad (1)$$

where $N_{\text{MOT}} = 2 \times 10^{10}$ is the number of muons on target (MOT), $n_{\text{Pb}} = 3.3 \times 10^{22} \text{ cm}^{-3}$ and $L_T = 20$ cm are the number density and thickness of the lead target [56]. Here conservatively we have ignored the contributions from the plastic scintillator layers of the ECAL. σ is the model-specific cross section, and κ the signal efficiency.

The efficiency depends on the effective mass of the bremsstrahlung particle, which we infer from the results in [56] and agrees with the shape in [57]. If the particle is off-shell, the effective mass is the momentum transfer to the particle $\sqrt{Q^2}$. If the dark particle is unstable, it may decay to final states that are visible or invisible to the calorimeters. For the former, missing energy is only fulfilled if the decay occurs either between calorimeters or beyond the last calorimeter. We therefore include the probability of invisible signal P_{inv} in this scenario. In the following, we will discuss the three models considered in this work.

III. AXION-PHOTON COUPLING

We first consider axion with photon coupling, which is common to QCD axions. The corresponding Lagrangian is

$$\mathcal{L} \supset \frac{1}{2}(\partial_\mu a)^2 - \frac{1}{2}m_a^2 a^2 - \frac{1}{4}g_{a\gamma\gamma} a F_{\mu\nu} \tilde{F}^{\mu\nu}, \quad (2)$$

where $F_{\mu\nu}$ denotes the strength tensor of the photon field and $\tilde{F}^{\mu\nu}$ is its dual $\tilde{F}^{\mu\nu} = \frac{1}{2}\epsilon^{\mu\nu\rho\sigma} F^{\rho\sigma}$. m_a and $g_{a\gamma\gamma}$ are axion mass and its coupling to photon.

As described in Fig. 1, axions are mainly produced through the photon-photon fusion. We use the Weizsäcker-Williams (WW) approximation [67–70], which simplifies the phase space integration of the $2 \rightarrow 3$ process by treating the virtual photon mediator that is attached to N as a real photon, reducing it to that of a $2 \rightarrow 2$ process. The approximation works well in the relativistic and collinear limit, particularly in the beam dump experiment [71] and for the purpose of this work [72]. Under the WW approximation, the differential cross section of the axion production process can be written as [71, 73]

$$\frac{d\sigma}{dx} = \frac{\alpha}{8\pi^2} \sqrt{E_a^2 - m_a^2} E_\mu (1-x) \int d\cos\theta \frac{\chi}{\tilde{u}^2} \mathcal{A}, \quad (3)$$

where $x = E_a/E_\mu$, θ is the angle between the dark state particle and the beam. Numerical study suggests that the integral could take the θ range from 0 to 0.1 [72]. \tilde{u} is the modified Mandelstam variable $\tilde{u} = (p_{\mu, \text{in}} - p_a)^2 - m_\mu^2 = -xE_\mu^2\theta^2 - m_a^2 \frac{1-x}{x} - m_\mu^2 x$, where $p_{\mu, \text{in}}$ and p_a are the four momenta of the incoming muon and outgoing axion. χ is the effective photon flux defined by

$$\chi = \int_{t_{\text{min}}}^{t_{\text{max}}} dt \frac{t - t_{\text{min}}}{t^2} F^2(t), \quad (4)$$

where the squared momentum transfer to the nucleus t varies between $t_{\text{min}} \approx \tilde{u}^2/(4E_\mu^2(1-x)^2)$ and $t_{\text{max}} \approx m_a^2 + m_\mu^2$ [74]. $F(t)$ is the elastic form factor of the nucleus [75]

$$F(t) \simeq Z \left(\frac{b^2 t}{1 + b^2 t} \right) \left(\frac{1}{1 + t/d} \right), \quad (5)$$

with $b = 111Z^{-1/3}/m_e$ and $d = 0.164 \text{ GeV}^2 A^{-2/3}$. For lead target the atomic number $Z = 82$ and the mass number $A = 207.2$. \mathcal{A} is the spin summed and averaged matrix element of the $2 \rightarrow 2$ process in the limit $t = t_{\text{min}}$. For axion production through photon-photon fusion this is

$$\mathcal{A}_{a-\gamma} = -e^2 g_{a\gamma\gamma}^2 \tilde{u}^2 \frac{\tilde{u}x(2-x) + 2m_\mu^2 x^2 + m_a^2(1-x)(2-x)}{(m_a^2(1-x) + x\tilde{u})^2}. \quad (6)$$

We then compute the production of axion using Eq. (1). As axion is generated on-shell, $Q^2 = m_a^2$. It is worth mentioning that the energy loss of muon is negligible in the target [76], and we keep the incoming muon

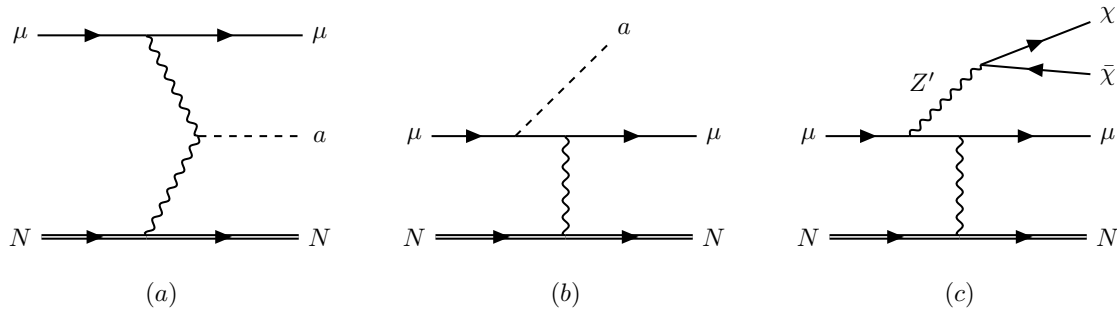


FIG. 1. Feynman diagrams for the production of dark particles in the NA64 μ experiment: (a) axion production through photon-photon fusion, (b) muophilic axion production through muon bremsstrahlung, and (c) a muon-philic dark sector where the dark particle χ is produced through a massless mediator Z' .

energy as a constant. The outgoing axion then leaves the target calorimeter and decay to photons. We focus on axions with mass $m_a \lesssim 0.1$ GeV. As axion with gauge boson coupling decays dominantly to photons [77], we neglect other decay channels, and count the events where axion decay past the veto in between calorimeters or beyond the last calorimeter. Although the axion production probability is uniform in the target, production location does affect the propagation distance before axion decay. We take this into consideration by summing up the decay probability for axion to be produced in different layers in the target, as detailed in Appendix A.

We then place constraints on axion-photon coupling at 90% CL by requiring the expect number of events from axion to be less than 2.3, using the current NA64 μ data. The results are shown in Fig. 2. We exclude the axion-photon coupling $g_{a\gamma\gamma} \gtrsim 3 \times 10^{-3}$ GeV $^{-1}$ for $m_a \lesssim 0.03$ GeV. It covers parameter space that was not covered by the previous NA64 electron beam dump [19]. The limit also exceeds the constraint obtained by recasting the LEP I data (labeled “LEP”) but is inferior to the recast of LEP II data (labeled “OPAL”) in the relevant axion mass range.

IV. AXION-MUON COUPLING

We also consider axion-like particles (ALPs) coupling to muons. The Lagrangian of for muon-philic ALP is given by

$$\mathcal{L} \supset \frac{1}{2}(\partial_\sigma a)^2 - \frac{1}{2}m_a^2 a^2 - ig_{a\mu\mu}(2m_\mu)\bar{\mu}\gamma_5\mu a, \quad (7)$$

where $g_{a\mu\mu}$ is the ALP-muon coupling. Under WW approximation, the differential cross section for axion production in muon bremsstrahlung is also given by Eq. (3), with the matrix element

$$\mathcal{A}_{a-\mu} = 4e^2 g_{a\mu\mu}^2 m_\mu^2 \left[\frac{x^2}{1-x} + 2m_a^2 \frac{\tilde{u}x + m_a^2(1-x) + m_\mu^2 x^2}{\tilde{u}^2} \right] \quad (8)$$

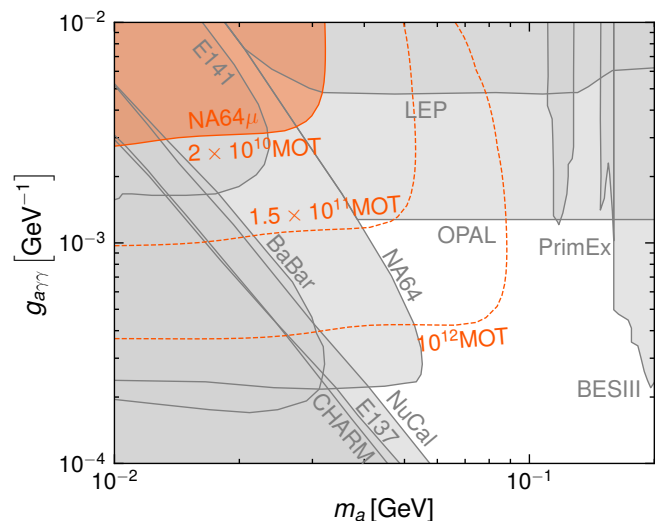


FIG. 2. 90% C.L. limits on the axion-photon coupling with the current NA64 μ data (red shaded region), and the projected sensitivity with 1.5×10^{11} and 10^{12} muon on target (dashed red lines). Existing constraints from collider and beam dump experiments are shown as grey shaded regions, including LEP [78], OPAL [21], PrimEx [79], BESIII [80, 81], E141 [82], NA64 electron beam dump [19], BaBar [83], NuCal [84], E137 [85] and CHARM [86].

The constraints on axion-muon coupling are shown in Fig. 3. For $m_a < 2m_\mu$, axion decay to muons is kinematically forbidden. In the absence of direct coupling to other SM particles, the decay to other particles is loop suppressed. Consequently the produced axions are long-lived which will not deposit energy in the detector, consistent with the signal region in this work. Heavier axion dominantly decays to two muons. Since axions are highly realistic, the two muons could be collinear and identified as a single muon. However, conservatively, we require axion to decay beyond the last HCAL calorimeter. The resultant sensitivity is not competitive and outside the scope of the figure. A similar pseudoscalar model is con-

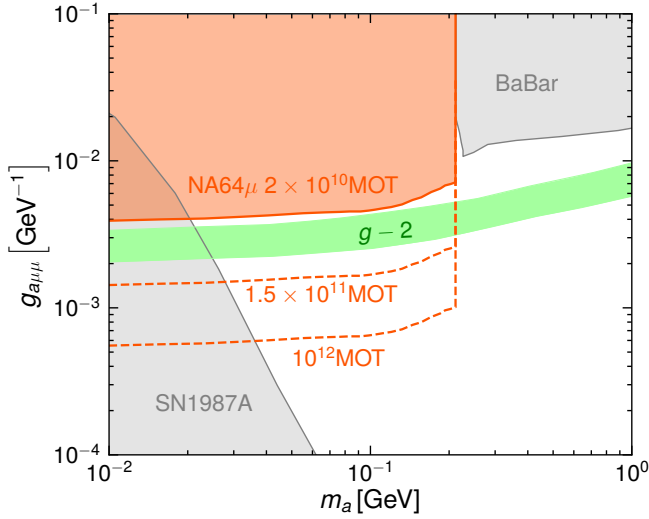


FIG. 3. Same as Fig. 2 but for axion-muon coupling. Existing constraints are shown as grey shaded regions, including BaBar [87] and SN1987A [88, 89]. The $(g-2)_\mu$ 2σ band is also shown as the green band [35].

sidered in [72] where the sensitivity is projected assuming the pseudoscalar decays to dark sector particles without the inclusion of the efficiency.

The NA64 μ experiment with its current exposure could exclude large parameter space for $m_a \lesssim 0.2$ GeV, which is at the margin of the axion parameter space that could explain the muon $g-2$ anomaly. Lower axion-muon coupling is constrained by the cooling of SN1987A [88]. At higher mass it is constrained by four-muon final states at BaBar [87].

V. MUON-PHILIC DARK SECTOR

Finally we consider the coupling between muon and the dark sector through a massless mediator. This is analogous to millicharged particles where the dark sector particles are lightly coupled to photon and can be produced through the bremsstrahlung of charged particles. We now introduce a muon-philic mediator so that the dark particle χ is preferably produced in muon scattering, while the coupling of χ to other particles is loop suppressed. This could be realized through a scalar or vector mediator. For concreteness, we consider the vector mediator to be a $L_\mu - L_\tau$ gauge boson, the interaction Lagrangian is given by

$$\mathcal{L} \supset g_{Z'} J_{\mu-\tau}^\sigma Z'_\sigma + g_\chi \bar{\chi} \not{Z}' \chi \quad (9)$$

with

$$J_{\mu-\tau}^\sigma = \bar{\mu} \gamma^\sigma \mu + \bar{\nu}_{\mu L} \gamma^\sigma \nu_{\mu L} - \bar{\tau} \gamma^\sigma \tau - \bar{\nu}_{\tau L} \gamma^\sigma \nu_{\tau L} \quad (10)$$

where the massless gauge boson Z' interacts with the dark fermion χ via coupling g_χ , and $g_{Z'}$ is the coupling of Z' to the second and third generation leptons.

As in Fig. 1, χ is produced in the $2 \rightarrow 4$ process $\mu N \rightarrow \mu N \chi \bar{\chi}$. The differential cross section of this process can be written as [90]

$$d\sigma(\mu N \rightarrow \mu N \chi \bar{\chi}) = d\sigma(\mu N \rightarrow \mu N Z') \times \frac{g_\chi^2}{12\pi^2} \frac{dQ^2}{Q^2} \sqrt{1 - \frac{4m_\chi^2}{Q^2}} \left(1 + \frac{2m_\chi^2}{Q^2}\right), \quad (11)$$

where $d\sigma(\mu N \rightarrow \mu N Z')$ is the differential cross section with a virtual Z' in the final state, and Q^2 the squared 4-momentum of the virtual Z' . Likewise, $d\sigma(\mu N \rightarrow \mu N Z')$ is given by Eq. (3) with E_a replaced by $E_{Z'}$ and m_a^2 replaced by Q^2 . The matrix element is now

$$\mathcal{A}_{Z'-\chi} = 4e^2 g_{Z'}^2 \left[\frac{x^2 - 2x + 2}{2(1-x)} + \frac{Q^2 + 2m_\mu^2}{\tilde{u}} + \frac{2m_\mu^4 x^2 + Q^4(1-x) + m_\mu^2 Q^2(x^2 - 2x + 2)}{\tilde{u}^2} \right], \quad (12)$$

where $\tilde{u} = -xE_\mu^2 \theta^2 - Q^2 \frac{1-x}{x} - m_\mu^2 x$. Since the dark fermion is invisible to the calorimeters, $P_{\text{inv}} = 1$ for the whole mass range we consider.

The constraint obtained from the current NA64 μ data is shown in Fig. 4. The constraint is compared with existing experiments, where χ is produced in electron or proton collisions through electromagnetic or weak interaction. The SM photon couples to Z' through the muon and tau loop, with the effective kinetic mixing [91]

$$\Pi(q^2) = \frac{eg_{Z'}}{2\pi^2} \int_0^1 dx (1-x) \ln \frac{m_\tau^2 - x(1-x)q^2}{m_\mu^2 - x(1-x)q^2}. \quad (13)$$

By redefining the field to remove the kinetic mixing, χ couples to photon direct with the interaction $\mathcal{L}_{\text{int}} \supset g_\chi \Pi(q^2) \bar{\chi} \not{A} \chi$. Therefore, the dark fermion χ can be seen as millicharged particle in these production processes. In the original millicharge model, if the dark particle carries the charge ϵe , it is equivalent to the muon-philic model with the coupling $g_{Z'} g_\chi = \epsilon e g_{Z'}/\Pi(q^2)$. For massless mediator, the production of χ is dominated by the minimum possible momentum transfer allowed by kinematics. We then choose $q^2 = 4m_\chi^2$ when recasting the constraint from ϵe to $g_{Z'} g_\chi$.

Although existing experiments have placed strong constraints on the dark particle millicharge, the sensitivity is lost severely by introducing the loop to interact with muon in the muon-philic model. The current NA64 μ data leads to more stringent constraints on $(g_{Z'} g_\chi)^2$ than existing ones by up to more than an order of magnitude in the mass range $m_\chi \lesssim 1$ GeV.

VI. CONCLUSIONS AND PROSPECTS

We have demonstrated the potential of exploring BSM physics, in particular muon-philic physics with a muon

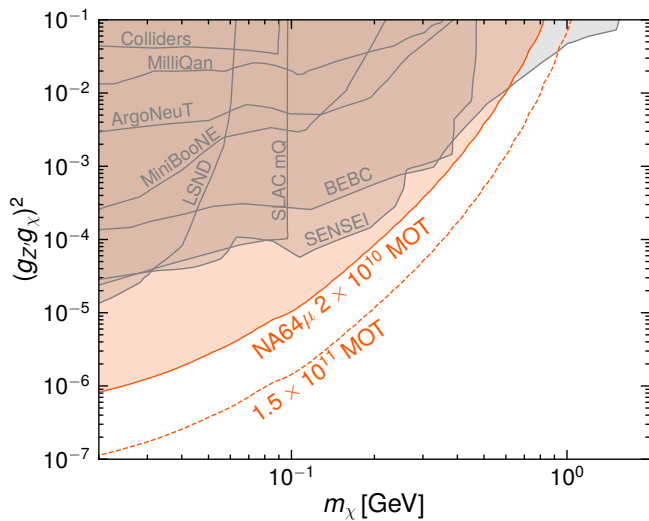


FIG. 4. Same as Fig. 2 but for a muon-philic dark sector. We recast the existing limits of millicharged particles in the grey shade regions, including Colliders [46], MilliQan [49], ArgoNeuT [92], MiniBooNE [43], LSND [43], SLAC mQ [41], BEBC [93] and SENSEI [94].

beam dump experiment. The current NA64 μ experiment with its pilot run has already achieved superior constraints than previous experiments. Following the 2022 run, a new run with 1.5×10^{11} MOT has been conducted at CERN utilizing better magnet spectrometer, detection and trigger systems in 2023. NA64 μ plans to accumulate 10^{12} MOT before the long shutdown to explore more parameter space [95], and finally reach the goal of 10^{14} MOT [57].

We present the projected sensitivity for the 2023 run (1.5×10^{11} MOT) and for 10^{12} MOT at NA64 μ with a similar experimental setup in Fig. 2 through Fig. 4. The axion-photon coupling does not scale linearly as $N_{\text{MOT}}^{-1/2}$ as the coupling also affects the lifetime of axion. More muons in the beam allow probing axion mass up to about 0.08 GeV at $g_{a\gamma\gamma} \sim 4 \times 10^{-4}$ GeV with 10^{12} MOT, as massive axions live longer with smaller coupling to be invisible. Even with the 2023 run, new parameter space will start to be excluded between NA64e and OPAL. Although we focus on the missing energy signature, axions decaying past the veto in the calorimeters could also be identified once the energy deposition information in each calorimeter is available, further improving the sensitivity [96].

The 2023 run also allows to rule out the muon $g-2$ parameter space for $m_a \lesssim 0.2$ GeV and 10^{12} MOT could exclude $g_{a\mu\mu} \gtrsim 5.5 \times 10^{-4}$ GeV $^{-1}$. Axion could also decay before the last calorimeters, yielding a muon pair that can be identified in the tracker, a smoking-gun signature of axion coupling with muons. We will investigate this possibility in future work.

For a muon-philic dark sector, the sensitivity on $(g_Z g_\chi)^2$ simple scales as N_{MOT}^{-1} . The 2023 run (10^{12}

MOT) will lead to about one (two) order of magnitude enhancement in the sensitivity.

A muon beam dump also facilitates the searches for more BSM scenarios, such as flavor-violating interactions [33, 64–66, 97–99]. For example, a muon-to-tau transition will be followed by the subsequent tau decay in ECAL. If tau decays leptonically to a muon that passes the muon trackers, it will satisfy the trigger in NA64 μ . This represents one of the few ways to explore flavor transition involving a tau lepton. With the advent of muon beam dumps and the upcoming muon colliders, we are not just entering an era of precise study, but also opening the window to the possibilities of flavor-specific interactions.

ACKNOWLEDGEMENT

We thank Paolo Crivelli and Laura Molina Bueno for useful correspondence on the NA64 μ experiment. HL and ZL are supported by the National Natural Science Foundation of China (NSFC) under Grant Nos. 12275128 and 12147103. NS is supported by the NSFC Project No. 12475110, No. 12347105 and No. 12047503.

Appendix A: Decay probability of long-lived axion

The ECAL consists of 150 layers of lead and plastic scintillator (Sc) plates [57]. Each layer contains 1.5 mm thick lead and 1.5 mm thick Sc, which combine into $40X_0$ of lead with $X_0 = 0.56$ cm. Among them, $4X_0$ are pre-shower detector, resulting in a net target length of $L_T = 20.16$ cm for muon scattering [100]. We assume that the probability of scattering in each layer of lead is the same. This is reasonable given the small energy loss of muon in ECAL (about 0.5 GeV) [101].

If axion is produced in the last layer of ECAL, the probability for axion to decay in between the calorimeters (i.e. invisible decay) is

$$P_0 = (1 - e^{-L_V/l_a}) + e^{-(L_H+2L_{\text{HCAL}})/l_a} + (e^{-(L_V+L_{\text{VHCAL}})/l_a} - e^{-L_H/l_a}), \quad (\text{A1})$$

where we have ignored the uncertainty for the location of the muon scattering inside the last layer. $L_V = 1.2$ m and $L_H = 6.85$ m are the distance from the end of the ECAL to the front of the VHCAL and the first HCAL, respectively. $L_{\text{VHCAL}} = 1$ m, $L_{\text{HCAL}} = 1.54$ m are the length of VHCAL and HCAL [57].

Labeling the layer from the last layer to the front as the 0th to the 135th layer (excluding the pre-shower layers), the invisible decay probability of axion in the k -th layer is $P_k = e^{-kd_0/l_a} P_0$, with $d_0 = 3$ mm the thickness of one lead-Sc layer. With the assumption that the probability of scattering in each later is the same, we can find the average invisible decay probability as $\bar{P}_{\text{inv}} = \frac{1}{136} \sum_{k=0}^{135} P_k$.

Appendix B: Virtual photon flux

The virtual photon flux in Eq. (4) can be integrated out as

$$\chi = Z^2 \frac{b^4 d^2}{(-1 + b^2 d)^3} (\chi_1 + \chi_2), \quad (\text{B1})$$

where

$$\begin{aligned} \chi_1 &= \frac{(-1 + b^2 d)(1 + b^2(d + 2t_{\max}))(t_{\max} - t_{\min})}{(d + t_{\max})(1 + b^2 t_{\max})}, \\ \chi_2 &= (1 + b^2(d + 2t_{\min})) \ln \left[\frac{(d + t_{\max})(1 + b^2 t_{\min})}{(d + t_{\min})(1 + b^2 t_{\max})} \right]. \end{aligned} \quad (\text{B2})$$

-
- * 502022220006@smail.nju.edu.cn
† zuoweiliu@nju.edu.cn
‡ songnq@itp.ac.cn
- [1] R. D. Peccei and H. R. Quinn, CP Conservation in the Presence of Instantons, *Phys. Rev. Lett.* **38**, 1440 (1977).
- [2] R. D. Peccei and H. R. Quinn, Constraints Imposed by CP Conservation in the Presence of Instantons, *Phys. Rev. D* **16**, 1791 (1977).
- [3] S. Weinberg, A New Light Boson?, *Phys. Rev. Lett.* **40**, 223 (1978).
- [4] F. Wilczek, Problem of Strong P and T Invariance in the Presence of Instantons, *Phys. Rev. Lett.* **40**, 279 (1978).
- [5] J. Preskill, M. B. Wise, and F. Wilczek, Cosmology of the Invisible Axion, *Phys. Lett. B* **120**, 127 (1983).
- [6] L. F. Abbott and P. Sikivie, A Cosmological Bound on the Invisible Axion, *Phys. Lett. B* **120**, 133 (1983).
- [7] M. Dine and W. Fischler, The Not So Harmless Axion, *Phys. Lett. B* **120**, 137 (1983).
- [8] L. D. Duffy and K. van Bibber, Axions as Dark Matter Particles, *New J. Phys.* **11**, 105008 (2009), [arXiv:0904.3346 \[hep-ph\]](#).
- [9] P. Arias, D. Cadamuro, M. Goodsell, J. Jaeckel, J. Redondo, and A. Ringwald, WISPy Cold Dark Matter, *JCAP* **06**, 013, [arXiv:1201.5902 \[hep-ph\]](#).
- [10] Y. K. Semertzidis and S. Youn, Axion dark matter: How to see it?, *Sci. Adv.* **8**, abm9928 (2022), [arXiv:2104.14831 \[hep-ph\]](#).
- [11] F. Chadha-Day, J. Ellis, and D. J. E. Marsh, Axion dark matter: What is it and why now?, *Sci. Adv.* **8**, abj3618 (2022), [arXiv:2105.01406 \[hep-ph\]](#).
- [12] Y. Gu, L. Wu, and B. Zhu, Axion dark radiation: Hubble tension and the Hyper-Kamiokande neutrino experiment, *Phys. Rev. D* **105**, 095008 (2022), [arXiv:2105.07232 \[hep-ph\]](#).
- [13] E. Witten, Some Properties of $O(32)$ Superstrings, *Phys. Lett. B* **149**, 351 (1984).
- [14] P. Svrcek and E. Witten, Axions In String Theory, *JHEP* **06**, 051, [arXiv:hep-th/0605206](#).
- [15] A. Arvanitaki, S. Dimopoulos, S. Dubovsky, N. Kaloper, and J. March-Russell, String Axiverse, *Phys. Rev. D* **81**, 123530 (2010), [arXiv:0905.4720 \[hep-th\]](#).
- [16] S. J. Asztalos *et al.* (ADMX), A SQUID-based microwave cavity search for dark-matter axions, *Phys. Rev. Lett.* **104**, 041301 (2010), [arXiv:0910.5914 \[astro-ph.CO\]](#).
- [17] N. Du *et al.* (ADMX), A Search for Invisible Axion Dark Matter with the Axion Dark Matter Experiment, *Phys. Rev. Lett.* **120**, 151301 (2018), [arXiv:1804.05750 \[hep-ex\]](#).
- [18] C. Bartram *et al.* (ADMX), Search for Invisible Axion Dark Matter in the 3.3–4.2 μeV Mass Range, *Phys. Rev. Lett.* **127**, 261803 (2021), [arXiv:2110.06096 \[hep-ex\]](#).
- [19] D. Banerjee *et al.* (NA64), Search for Axionlike and Scalar Particles with the NA64 Experiment, *Phys. Rev. Lett.* **125**, 081801 (2020), [arXiv:2005.02710 \[hep-ex\]](#).
- [20] F. Abudinén *et al.* (Belle-II), Search for Axion-Like Particles produced in e^+e^- collisions at Belle II, *Phys. Rev. Lett.* **125**, 161806 (2020), [arXiv:2007.13071 \[hep-ex\]](#).
- [21] S. Knapen, T. Lin, H. K. Lou, and T. Melia, Searching for Axionlike Particles with Ultraperipheral Heavy-Ion Collisions, *Phys. Rev. Lett.* **118**, 171801 (2017), [arXiv:1607.06083 \[hep-ph\]](#).
- [22] M. Ajello *et al.* (Fermi-LAT), Search for Spectral Irregularities due to Photon–Axionlike-Particle Oscillations with the Fermi Large Area Telescope, *Phys. Rev. Lett.* **116**, 161101 (2016), [arXiv:1603.06978 \[astro-ph.HE\]](#).
- [23] J. W. Foster, S. J. Witte, M. Lawson, T. Linden, V. Gajjar, C. Weniger, and B. R. Safdi, Extraterrestrial Axion Search with the Breakthrough Listen Galactic Center Survey, *Phys. Rev. Lett.* **129**, 251102 (2022), [arXiv:2202.08274 \[astro-ph.CO\]](#).
- [24] N. Song, L. Su, and L. Wu, Polarization Signals from Axion-Photon Resonant Conversion in Neutron Star Magnetosphere, (2024), [arXiv:2402.15144 \[hep-ph\]](#).
- [25] D. P. Aguillard *et al.* (Muon g-2), Measurement of the Positive Muon Anomalous Magnetic Moment to 0.20 ppm, *Phys. Rev. Lett.* **131**, 161802 (2023), [arXiv:2308.06230 \[hep-ex\]](#).
- [26] B. Abi *et al.* (Muon g-2), Measurement of the Positive Muon Anomalous Magnetic Moment to 0.46 ppm, *Phys. Rev. Lett.* **126**, 141801 (2021), [arXiv:2104.03281 \[hep-ex\]](#).
- [27] T. Aoyama *et al.*, The anomalous magnetic moment of the muon in the Standard Model, *Phys. Rept.* **887**, 1 (2020), [arXiv:2006.04822 \[hep-ph\]](#).

- [28] S. Borsanyi *et al.*, Leading hadronic contribution to the muon magnetic moment from lattice QCD, *Nature* **593**, 51 (2021), [arXiv:2002.12347 \[hep-lat\]](#).
- [29] A. Boccaletti *et al.*, High precision calculation of the hadronic vacuum polarisation contribution to the muon anomaly, (2024), [arXiv:2407.10913 \[hep-lat\]](#).
- [30] D. Chang, W.-F. Chang, C.-H. Chou, and W.-Y. Keung, Large two loop contributions to $g-2$ from a generic pseudoscalar boson, *Phys. Rev. D* **63**, 091301 (2001), [arXiv:hep-ph/0009292](#).
- [31] W. J. Marciano, A. Masiero, P. Paradisi, and M. Passera, Contributions of axionlike particles to lepton dipole moments, *Phys. Rev. D* **94**, 115033 (2016), [arXiv:1607.01022 \[hep-ph\]](#).
- [32] M. Bauer, M. Neubert, and A. Thamm, Collider Probes of Axion-Like Particles, *JHEP* **12**, 044, [arXiv:1708.00443 \[hep-ph\]](#).
- [33] M. Bauer, M. Neubert, S. Renner, M. Schnubel, and A. Thamm, Axionlike Particles, Lepton-Flavor Violation, and a New Explanation of a_μ and a_e , *Phys. Rev. Lett.* **124**, 211803 (2020), [arXiv:1908.00008 \[hep-ph\]](#).
- [34] C. Cornella, P. Paradisi, and O. Sumensari, Hunting for ALPs with Lepton Flavor Violation, *JHEP* **01**, 158, [arXiv:1911.06279 \[hep-ph\]](#).
- [35] M. A. Buen-Abad, J. Fan, M. Reece, and C. Sun, Challenges for an axion explanation of the muon $g - 2$ measurement, *JHEP* **09**, 101, [arXiv:2104.03267 \[hep-ph\]](#).
- [36] B. Holdom, Two U(1)'s and Epsilon Charge Shifts, *Phys. Lett. B* **166**, 196 (1986).
- [37] R. Foot and X.-G. He, Comment on Z Z-prime mixing in extended gauge theories, *Phys. Lett. B* **267**, 509 (1991).
- [38] C. Cheung, J. T. Ruderman, L.-T. Wang, and I. Yavin, Kinetic Mixing as the Origin of Light Dark Scales, *Phys. Rev. D* **80**, 035008 (2009), [arXiv:0902.3246 \[hep-ph\]](#).
- [39] T. Gherghetta, J. Kersten, K. Olive, and M. Pospelov, Evaluating the price of tiny kinetic mixing, *Phys. Rev. D* **100**, 095001 (2019), [arXiv:1909.00696 \[hep-ph\]](#).
- [40] D. Feldman, Z. Liu, and P. Nath, The Stueckelberg Z-prime Extension with Kinetic Mixing and Milli-Charged Dark Matter From the Hidden Sector, *Phys. Rev. D* **75**, 115001 (2007), [arXiv:hep-ph/0702123](#).
- [41] A. A. Prinz *et al.*, Search for millicharged particles at SLAC, *Phys. Rev. Lett.* **81**, 1175 (1998), [arXiv:hep-ex/9804008](#).
- [42] E. Golowich and R. W. Robinett, Limits on Millicharged Matter From Beam Dump Experiments, *Phys. Rev. D* **35**, 391 (1987).
- [43] G. Magill, R. Plestid, M. Pospelov, and Y.-D. Tsai, Millicharged particles in neutrino experiments, *Phys. Rev. Lett.* **122**, 071801 (2019), [arXiv:1806.03310 \[hep-ph\]](#).
- [44] R. Harnik, Z. Liu, and O. Palamara, Millicharged Particles in Liquid Argon Neutrino Experiments, *JHEP* **07**, 170, [arXiv:1902.03246 \[hep-ph\]](#).
- [45] S. Davidson, B. Campbell, and D. C. Bailey, Limits on particles of small electric charge, *Phys. Rev. D* **43**, 2314 (1991).
- [46] S. Davidson, S. Hannestad, and G. Raffelt, Updated bounds on millicharged particles, *JHEP* **05**, 003, [arXiv:hep-ph/0001179](#).
- [47] Z. Liu and Y. Zhang, Probing millicharge at BESIII via monophoton searches, *Phys. Rev. D* **99**, 015004 (2019), [arXiv:1808.00983 \[hep-ph\]](#).
- [48] J. Liang, Z. Liu, Y. Ma, and Y. Zhang, Millicharged particles at electron colliders, *Phys. Rev. D* **102**, 015002 (2020), [arXiv:1909.06847 \[hep-ph\]](#).
- [49] A. Ball *et al.*, Search for millicharged particles in proton-proton collisions at $\sqrt{s} = 13$ TeV, *Phys. Rev. D* **102**, 032002 (2020), [arXiv:2005.06518 \[hep-ex\]](#).
- [50] R. Plestid, V. Takhistov, Y.-D. Tsai, T. Bringmann, A. Kusenko, and M. Pospelov, New Constraints on Millicharged Particles from Cosmic-ray Production, *Phys. Rev. D* **102**, 115032 (2020), [arXiv:2002.11732 \[hep-ph\]](#).
- [51] M. Kachelriess and J. Tjemsland, Meson production in air showers and the search for light exotic particles, *Astropart. Phys.* **132**, 102622 (2021), [arXiv:2104.06811 \[hep-ph\]](#).
- [52] C. A. Argüelles Delgado, K. J. Kelly, and V. Muñoz Alborno, Millicharged particles from the heavens: single- and multiple-scattering signatures, *JHEP* **11**, 099, [arXiv:2104.13924 \[hep-ph\]](#).
- [53] H. Wu, E. Hardy, and N. Song, Searching for heavy millicharged particles from the atmosphere, (2024), [arXiv:2406.01668 \[hep-ph\]](#).
- [54] M. Du, R. Fang, and Z. Liu, Millicharged particles from proton bremsstrahlung in the atmosphere, *JHEP* **08**, 174, [arXiv:2211.11469 \[hep-ph\]](#).
- [55] M. Du, R. Fang, Z. Liu, W. Lu, and Z. Ye, Probing invisible dark photon models via atmospheric collisions, (2023), [arXiv:2308.05607 \[hep-ph\]](#).
- [56] Y. M. Andreev *et al.* (NA64), First Results in the Search for Dark Sectors at NA64 with the CERN SPS High Energy Muon Beam, *Phys. Rev. Lett.* **132**, 211803 (2024), [arXiv:2401.01708 \[hep-ex\]](#).
- [57] Y. M. Andreev *et al.*, Shedding light on Dark Sectors with high-energy muons at the NA64 experiment at the CERN SPS, (2024), [arXiv:2409.10128 \[hep-ex\]](#).
- [58] W. Altmannshofer, S. Gori, and G. D. Kribs, A Minimal Flavor Violating 2HDM at the LHC, *Phys. Rev. D* **86**, 115009 (2012), [arXiv:1210.2465 \[hep-ph\]](#).
- [59] W. Altmannshofer, S. Gori, A. L. Kagan, L. Silvestrini, and J. Zupan, Uncovering Mass Generation Through Higgs Flavor Violation, *Phys. Rev. D* **93**, 031301 (2016), [arXiv:1507.07927 \[hep-ph\]](#).
- [60] J. A. Evans, D. Shih, and A. Thalappilil, Chiral Flavor Violation from Extended Gauge Mediation, *JHEP* **07**, 040, [arXiv:1504.00930 \[hep-ph\]](#).
- [61] M. Bauer, M. Carena, and K. Gemmler, Flavor from the Electroweak Scale, *JHEP* **11**, 016, [arXiv:1506.01719 \[hep-ph\]](#).
- [62] P. Coloma, M. C. Gonzalez-Garcia, and M. Maltoni, Neutrino oscillation constraints on U(1)' models: from non-standard interactions to long-range forces, *JHEP* **01**, 114, [Erratum: *JHEP* **11**, 115 (2022)], [arXiv:2009.14220 \[hep-ph\]](#).
- [63] S. Gninenko and D. Gorbunov, Refining constraints from Borexino measurements on a light Z' -boson coupled to L_μ - L_τ current, *Phys. Lett. B* **823**, 136739 (2021), [arXiv:2007.16098 \[hep-ph\]](#).
- [64] M. Bauer, P. Foldenauer, and M. Mosny, Flavor structure of anomaly-free hidden photon models, *Phys. Rev. D* **103**, 075024 (2021), [arXiv:2011.12973 \[hep-ph\]](#).
- [65] M. Bauer, M. Neubert, S. Renner, M. Schnubel, and A. Thamm, Flavor probes of axion-like particles, *JHEP* **09**, 056, [arXiv:2110.10698 \[hep-ph\]](#).
- [66] B. Batell, H. Davoudiasl, R. Marcarelli, E. T. Neil, and S. Trojanowski, Lepton-flavor-violating ALP signals with TeV-scale muon beams, *Phys. Rev. D* **110**, 075039 (2024), [arXiv:2407.15942 \[hep-ph\]](#).

- [67] C. F. von Weizsacker, Radiation emitted in collisions of very fast electrons, *Z. Phys.* **88**, 612 (1934).
- [68] E. J. Williams, Correlation of certain collision problems with radiation theory, (No Title) (1935).
- [69] K. J. Kim and Y.-S. Tsai, IMPROVED WEIZSACKER-WILLIAMS METHOD AND ITS APPLICATION TO LEPTON AND W BOSON PAIR PRODUCTION, *Phys. Rev. D* **8**, 3109 (1973).
- [70] Y.-S. Tsai, Pair Production and Bremsstrahlung of Charged Leptons, *Rev. Mod. Phys.* **46**, 815 (1974), [Erratum: *Rev. Mod. Phys.* 49, 421–423 (1977)].
- [71] Y.-S. Liu and G. A. Miller, Validity of the Weizsäcker-Williams approximation and the analysis of beam dump experiments: Production of an axion, a dark photon, or a new axial-vector boson, *Phys. Rev. D* **96**, 016004 (2017), [arXiv:1705.01633 \[hep-ph\]](#).
- [72] H. Sieber, D. V. Kirpichnikov, I. V. Voronchikhin, P. Crivelli, S. N. Gninenko, M. M. Kirsanov, N. V. Krasnikov, L. Molina-Bueno, and S. K. Sekatskii, Probing hidden sectors with a muon beam: Implication of spin-0 dark matter mediators for the muon ($g-2$) anomaly and the validity of the Weizsäcker-Williams approach, *Phys. Rev. D* **108**, 056018 (2023), [arXiv:2305.09015 \[hep-ph\]](#).
- [73] J. Liu, Y. Luo, and M. Song, Investigation of the concurrent effects of ALP-photon and ALP-electron couplings in Collider and Beam Dump Searches, *JHEP* **09**, 104, [arXiv:2304.05435 \[hep-ph\]](#).
- [74] D. V. Kirpichnikov, H. Sieber, L. M. Bueno, P. Crivelli, and M. M. Kirsanov, Probing hidden sectors with a muon beam: Total and differential cross sections for vector boson production in muon bremsstrahlung, *Phys. Rev. D* **104**, 076012 (2021), [arXiv:2107.13297 \[hep-ph\]](#).
- [75] J. D. Bjorken, R. Essig, P. Schuster, and N. Toro, New Fixed-Target Experiments to Search for Dark Gauge Forces, *Phys. Rev. D* **80**, 075018 (2009), [arXiv:0906.0580 \[hep-ph\]](#).
- [76] C.-Y. Chen, M. Pospelov, and Y.-M. Zhong, Muon Beam Experiments to Probe the Dark Sector, *Phys. Rev. D* **95**, 115005 (2017), [arXiv:1701.07437 \[hep-ph\]](#).
- [77] G. Alonso-Álvarez, M. B. Gavela, and P. Quilez, Axion couplings to electroweak gauge bosons, *Eur. Phys. J. C* **79**, 223 (2019), [arXiv:1811.05466 \[hep-ph\]](#).
- [78] J. Jaeckel and M. Spannowsky, Probing MeV to 90 GeV axion-like particles with LEP and LHC, *Phys. Lett. B* **753**, 482 (2016), [arXiv:1509.00476 \[hep-ph\]](#).
- [79] D. Aloni, C. Fanelli, Y. Soreq, and M. Williams, Photoproduction of Axionlike Particles, *Phys. Rev. Lett.* **123**, 071801 (2019), [arXiv:1903.03586 \[hep-ph\]](#).
- [80] M. Ablikim *et al.* (BESIII), Search for an axion-like particle in radiative J/ψ decays, *Phys. Lett. B* **838**, 137698 (2023), [arXiv:2211.12699 \[hep-ex\]](#).
- [81] M. Ablikim *et al.* (BESIII), Search for diphoton decays of an axionlike particle in radiative J/ψ decays, *Phys. Rev. D* **110**, L031101 (2024), [arXiv:2404.04640 \[hep-ex\]](#).
- [82] B. Döbrich, Axion-like Particles from Primakov production in beam-dumps, *CERN Proc.* **1**, 253 (2018), [arXiv:1708.05776 \[hep-ph\]](#).
- [83] M. J. Dolan, T. Ferber, C. Hearty, F. Kahlhoefer, and K. Schmidt-Hoberg, Revised constraints and Belle II sensitivity for visible and invisible axion-like particles, *JHEP* **12**, 094, [Erratum: *JHEP* 03, 190 (2021)], [arXiv:1709.00009 \[hep-ph\]](#).
- [84] J. Blumlein *et al.*, Limits on neutral light scalar and pseudoscalar particles in a proton beam dump experiment, *Z. Phys. C* **51**, 341 (1991).
- [85] J. D. Bjorken, S. Ecklund, W. R. Nelson, A. Abashian, C. Church, B. Lu, L. W. Mo, T. A. Nunamaker, and P. Rassmann, Search for Neutral Metastable Penetrating Particles Produced in the SLAC Beam Dump, *Phys. Rev. D* **38**, 3375 (1988).
- [86] F. Bergsma *et al.* (CHARM), Search for Axion Like Particle Production in 400-GeV Proton - Copper Interactions, *Phys. Lett. B* **157**, 458 (1985).
- [87] J. P. Lees *et al.* (BaBar), Search for a muonic dark force at BABAR, *Phys. Rev. D* **94**, 011102 (2016), [arXiv:1606.03501 \[hep-ex\]](#).
- [88] D. Croon, G. Elor, R. K. Leane, and S. D. McDermott, Supernova Muons: New Constraints on Z' Bosons, Axions and ALPs, *JHEP* **01**, 107, [arXiv:2006.13942 \[hep-ph\]](#).
- [89] R. Bollig, W. DeRocco, P. W. Graham, and H.-T. Janka, Muons in Supernovae: Implications for the Axion-Muon Coupling, *Phys. Rev. Lett.* **125**, 051104 (2020), [Erratum: *Phys. Rev. Lett.* 126, 189901 (2021)], [arXiv:2005.07141 \[hep-ph\]](#).
- [90] S. N. Gninenko, D. V. Kirpichnikov, and N. V. Krasnikov, Probing millicharged particles with NA64 experiment at CERN, *Phys. Rev. D* **100**, 035003 (2019), [arXiv:1810.06856 \[hep-ph\]](#).
- [91] T. Araki, S. Hoshino, T. Ota, J. Sato, and T. Shimomura, Detecting the $L_\mu - L_\tau$ gauge boson at Belle II, *Phys. Rev. D* **95**, 055006 (2017), [arXiv:1702.01497 \[hep-ph\]](#).
- [92] R. Acciarri *et al.* (ArgoNeuT), Improved Limits on Millicharged Particles Using the ArgoNeuT Experiment at Fermilab, *Phys. Rev. Lett.* **124**, 131801 (2020), [arXiv:1911.07996 \[hep-ex\]](#).
- [93] G. Marocco and S. Sarkar, Blast from the past: Constraints on the dark sector from the BEBC WA66 beam dump experiment, *SciPost Phys.* **10**, 043 (2021), [arXiv:2011.08153 \[hep-ph\]](#).
- [94] L. Barak *et al.* (SENSEI), Search by the SENSEI Experiment for Millicharged Particles Produced in the NuMI Beam, *Phys. Rev. Lett.* **133**, 071801 (2024), [arXiv:2305.04964 \[hep-ex\]](#).
- [95] T. N. Collaboration, NA64 Status Report 2023 (2023).
- [96] R. R. Dusaev, D. V. Kirpichnikov, and M. M. Kirsanov, Photoproduction of axionlike particles in the NA64 experiment, *Phys. Rev. D* **102**, 055018 (2020), [arXiv:2004.04469 \[hep-ph\]](#).
- [97] S. Gninenko, S. Kovalenko, S. Kuleshov, V. E. Lyubovitskij, and A. S. Zhevlovskov, Deep inelastic $e - \tau$ and $\mu - \tau$ conversion in the NA64 experiment at the CERN SPS, *Phys. Rev. D* **98**, 015007 (2018), [arXiv:1804.05550 \[hep-ph\]](#).
- [98] S. N. Gninenko and N. V. Krasnikov (NA64), Leptonic scalar portal: Origin of muon $g - 2$ anomaly and dark matter?, *Phys. Rev. D* **106**, 015003 (2022), [arXiv:2202.04410 \[hep-ph\]](#).
- [99] B. Radics, L. Molina-Bueno, L. Fields., H. Sieber, and P. Crivelli, Sensitivity potential to a light flavor-changing scalar boson with DUNE and NA64 μ , *Eur. Phys. J. C* **83**, 775 (2023), [arXiv:2306.07405 \[hep-ex\]](#).
- [100] H. H. Sieber, *Dark Sector Searches Weakly Coupled to Muons with the NA64 μ Experiment at CERN*, Ph.D. thesis, Zurich, ETH (2024).

- [101] D. E. Groom, N. V. Mokhov, and S. I. Striganov, Muon stopping power and range tables 10-MeV to 100-TeV, [Atom. Data Nucl. Data Tabl. **78**, 183 \(2001\)](#).